Journal of Thermal Analysis and Calorimetry (2024) 149:7551–7563
https://doi.org/10.1007/s10973-024-13292-4

Analysis of drying characteristics and quality attributes in peach slices dried via electrohydrodynamic, hot air and electrohydrodynamic-hot air methods

Ahmet Polat[1]

Received: 10 October 2023 / Accepted: 19 May 2024 / Published online: 23 July 2024

Abstract

This study aimed to investigate drying times mathematical models and assess the color, rehydration capacity, and microstructure of dried peach using electrohydrodynamic (EHD), hot air, and electrohydrodynamic-hot air (EHD-hot air) drying methods. Peach samples were subjected to drying with two different air temperatures (50 and 55 °C) and electric field (EF, 6.67 and 10 kV cm^{-1}) under constant air velocity (1.5 m s^{-1}). The longest drying durations were obtained in the EHD method (720 and 600 min), followed by hot air (290 and 260 min) and EHD-hot air method (120, 140, 170, and 200 min), respectively. The drying curves were best described by the Midilli et al. and Logarithmic models. The L^* values of the samples subjected to hot air drying were found to be lower than those obtained through other methods. No significant effect of the electric field on rehydration capacity was observed. The study revealed that increased temperature and electric field led to surface cracks on the peach. The study highlights the compatibility of the EHD method with the hot air method, suggesting its potential application within the drying industry. From these findings, it was seen that the EHD-hot air combination method could be an alternative to the hot air method in the food industry by reducing the drying time of peaches and considering that the color parameters are generally better than the hot air method.

Keywords Peach · Electrohydrodynamic · Color · Mathematical modeling · Microstructure

List of symbols

a^*	Color parameter indicative of the transition from green (+) to red (−)
b^*	Color parameter indicative of the transition from yellow (+) to blue (−)
C	Chroma
d	Distance/cm
EHD	Electrohydrodynamic
EF	Electric field/kV cm^{-1}
α°	Hue angle
ΔE	Total color differences
L^*	Lightness of a color
M_t	Moisture content at a given time t/g water g dry $matter^{-1}$
M_0	Initial moisture content/g water g dry $matter^{-1}$
M_e	Moisture content at equilibrium/g water g dry $matter^{-1}$
$MR_{exp,i}$	Experimental moisture ratio as measured
$MR_{pre.i}$	Predicted moisture ratio for the respective measurement
χ^2	Chi-square
$RMSE$	Root mean square error
R^2	Correlation coefficient
T	Drying air temperature/°C
t	Drying time/min
V	Voltage/kV
W_1	Mass of the dried product/g
W_2	Mass of rehydrated product/g

Subscripts

$a,b,K,k_o,g,c,k1$	Constant value
e	Equilibrium
o	Initial
N	Number of experimental data observed
Z	Number of the independent variable in the model

✉ Ahmet Polat
ahmetpolat@uludag.edu.tr

[1] Department of Biosystems Engineering, Faculty of Agriculture, Bursa Uludag University, Gorukle Campus, 16059 Bursa, Turkey

Introduction

It has been approximated that the aggregate losses incurred during the post-harvest stage of vegetables and fruits amount to 30–40% compared to the total production, constituting a significant contributing factor to the escalation of food costs [1]. Drying has long been employed as one of the oldest preservation methods to prevent such losses for fruits and vegetables typically harvested during specific seasons of the year, which begin to deteriorate after harvest and are challenging to store and transport. The drying process facilitates the reduction of water content from food substances, thereby mitigating the proliferation of microorganisms and averting spoilage. The attainment of a low residual water concentration within the product confers reduced susceptibility to microbial activity and curtails the extent of chemical and physical alterations during subsequent storage periods. By water removal, foods can be preserved for utilization during off-season periods, thereby shielding them against microbial deterioration and enzymatic transformations. In conventional drying processes, heat and mass transfer are increased using convective, conductive, and radial heat sources [2–4]. Convective air drying has emerged as the dominant method for product dehydration due to its ease of implementation. The main advantages of using hot air in drying processes are better removal of surface moisture and lower operational expenditure. This method finds widespread application in the dehydration of fruits and vegetables and requires the circulation of heated air across or over the product surface to ensure moisture removal. However, it was found that the presence of heat generated for drying the product in the system negatively affected the color, texture, aroma, and nutritional properties of the product [5, 6]. Furthermore, drying represents one of the most energy-intensive steps in food processing, resulting in high production costs. In consideration of these, recent researches have focused on developing new drying methods aimed at reducing drying time, enhancing product quality, and improving the system's overall energy efficiency [7]. One such innovative drying method is electrohydrodynamic drying technology. This approach relies on creating a high-voltage corona discharge to generate an ionic wind within the airflow. It involves establishing a substantial voltage difference between a grounded collector electrode and an emitter electrode, typically featuring a tiny radius wire or needle. As a result of this setup, the air near the emitter becomes ionized at high voltages, often reaching kilovolts. Ions are induced to migrate towards the collecting electrode under the influence of the Coulomb force. During the movement of the ions, they hit the neutral molecules in the air and transmit their momentum. With the change of momentum, an air movement called ionic wind occurs. This wind, created through the process, facilitates drying by enhancing heat and mass transfer between the product and the airflow [8]. The principal merit inherent in EHD drying technology resides in its non-thermal characteristics, rendering it especially well-suited for the efficient desiccation of heat-sensitive agricultural commodities. This innovative approach has demonstrated superiority over conventional mechanical air drying systems by avoiding the generation of vibrational disturbances, exhibiting a reduced response time, and displaying enhanced energy efficiency. In addition, it has another advantage over the fan system in terms of system and design since the airflow produced by EHD is created just below the needle, not from the center like fan dryers [9]. Furthermore, when analyzed in terms of final product quality, Alemrajabi et al. [10], Bai et al. [11], and Elmizadeh et al. [12] reported lower shrinkage ratios, higher rehydration capacity values, and improved color quality when employing the EHD method in comparison to conventional oven drying.

The botanical classification of peach (*Amygdalus persica* Linn) situates it within the Rosaceae family and the genus Prunus. Renowned for its rich nutritional profile, peaches are replete with vitamins, minerals, soluble dietary fiber, carotenoids, and proteins, among other bioactive constituents. They wield significant influence over individuals' daily dietary practices, enjoying widespread consumer popularity. The constituents contributing to the olfactory characteristics of foodstuffs are pivotal in discerning their quality and eventual acceptance by discerning consumers [13]. The drying process is applied to peach products for off-season consumption. Peach products are dried by different methods such as hot air, natural drying, freeze drying, far-infrared, microwave, hot air-microwave combined method, and sun drying, and there are many articles discussing the effects on different parameters [14–17]. According to the literature study, no studies were found on drying peach by EHD, hot air and EHD-hot air methods. In this study, the aim of the peach samples dried by EHD, hot air, and EHD-hot air methods is as follows:

- To perform a comparative analysis of quality parameters, explicitly focusing on color, shrinkage, rehydration, and microstructure across dried peach samples obtained via different drying methodologies.
- To identify the most suitable model for this specific investigation, the experimental dataset concerning the relationship between moisture ratio and drying time was analyzed using ten distinct mathematical models.

Materials and methods

Sample preparation

This study utilized peach (*Prunus persica* L.) fruit harvested from the Bursa region. The peach specimens were placed in a refrigeration unit, where a stable temperature of 4 ± 0.01 °C was maintained until the desiccation process reached its conclusion. Following the drying procedure, which involved exposing the products to a temperature of 70 °C for 24 h, the initial moisture content was assessed, yielding a value of 6.58 on a dry basis (d.b.). Subsequently, ripe and undamaged products retrieved from the refrigerator were allowed to attain room temperature, after which their skins were peeled and sliced using a specialized slicer. The average slice thickness and diameter of the products prepared for the experiments were measured with the caliper as 2.31 ± 0.13 and 53.21 ± 7.47 mm, respectively.

Experimental setup

Figure 1 shows the EHD-hot air combination oven used for drying peach samples. In the EHD system, six wires (0.04 mm diameter) were placed at 50 mm intervals [5]. The hot air arrival direction and the placement of the EHD wire system are positioned opposite each other. In this study, peach samples were dried by EHD (EF: 6.67, and 10 kV cm^{-1}), hot air (50 and 55 °C), and EHD-hot air combination (EF6.67–50 °C, EF6.67–55 °C, EF10-50 °C, and EF10-55 °C) methods. The electric field parameter in the table was created by calculating the distance between the products and the high voltage Eq. (1). In Eq. (1), V represents the applied voltage, while d is the distance between the wire and the product.

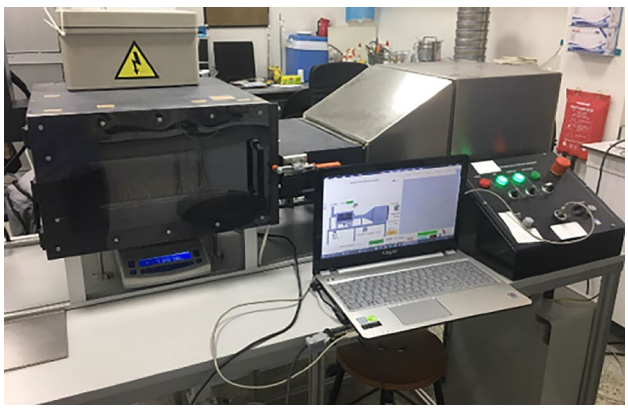

Fig. 1 EHD-hot air combination oven

$$EF = \frac{V(kV)}{d(cm)} \tag{1}$$

All experimental treatments were carried out within controlled laboratory settings, with an air velocity of 1.5 (m s^{-1}), while maintaining a consistent temperature of 26 °C and a relative humidity level of 24%. For each experiment, a stainless steel plate holding 130 ± 0.1 g of fresh peach samples was positioned within the oven. Moisture loss was monitored by measuring at 10-min intervals using a precise balance situated at the base of the oven until the equilibrium moisture content, accurate to 0.1 d.b., was attained. These experiments were conducted in triplicate.

Mathematical modeling of drying data

In the modeling studies, the moisture content values of peach samples with an average thickness of 2.31 ± 0.13 mm and diameter of 53.21 ± 7.47 mm, round and dry basis of 6.58 were converted into moisture ratio values. Figure 2 shows the flowchart of the modeling. The experimental data obtained by drying the peach samples subjected to EHD, hot air, and EHD-hot air combination were modeled using the thin layer drying model in Table 1, which is most widely used in the literature. The dimensionless moisture ratio values were computed employing Eq. (2) [18].

$$MR = \frac{M_t - M_e}{M_o - M_e} \tag{2}$$

Within the formula mentioned above, the variables M_t, M_0, and M_e denote the moisture content at a given time t (g water g dry $matter^{-1}$), the initial moisture content (g water g dry $matter^{-1}$), and the moisture content at equilibrium (g water g dry $matter^{-1}$), respectively. Since the M_e value is smaller than the M_t and M_0 values in some studies, the M_e value in Eq. (2) is neglected, and Eq. (3) is used [29]:

$$MR = \frac{M_t}{M_o} \tag{3}$$

Color measurement

The surface color analysis of both fresh and dehydrated peach slices was conducted using a colorimeter (MSEZ-4500 L, HunterLab, USA). Prior to acquiring color values for the products, the instrument underwent a calibration process using standard black and white plates. Color measurements were executed based on the L^*, a^*, and b^* coordinate system, following the principles of the CIELab color system. In this system, L^* signifies the luminance or lightness of a

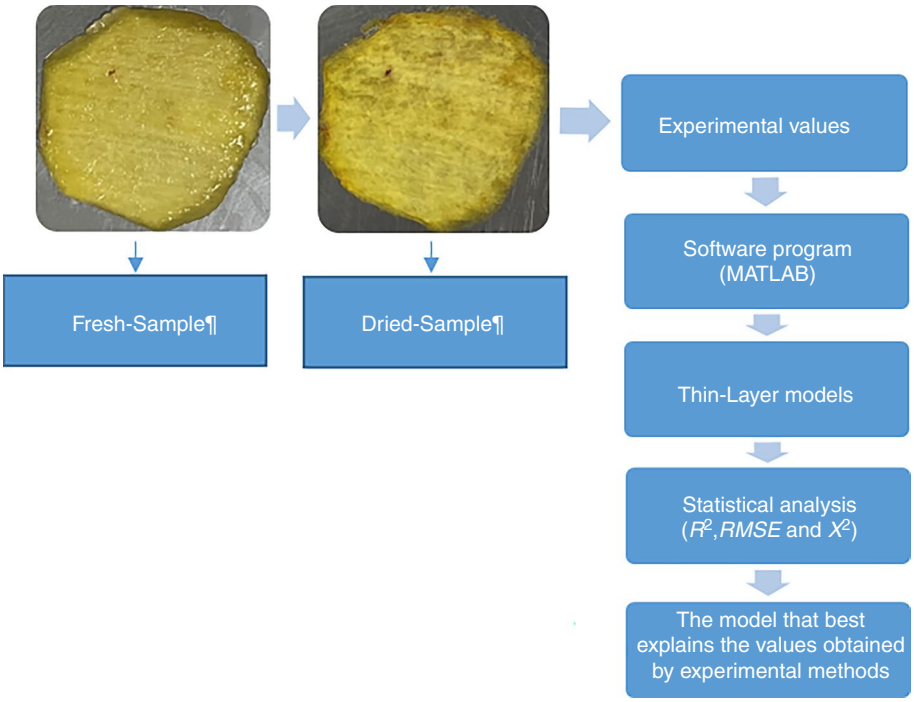

Fig. 2 The flowchart of the modeling

Table 1 Thin layer mathematical modeling equations to be used for the comparison of the moisture ratio values

No	Model name	Model	References
1	Henderson and Pabis	$MR = a\exp(-kt)$	[19]
2	Newton	$MR = \exp(-kt)$	[20]
3	Page	$MR = \exp(-kt^n)$	[21]
4	Logarithmic	$MR = a\exp(-kt) + c$	[22]
5	Two term	$MR = a\exp(-k_0t) + b\exp(-k_1t)$	[23]
6	Two term exponential	$MR = a\exp(-kt) + (1-a)\exp(-kat)$	[24]
7	Wang and Singh	$MR = 1 + at + bt^2$	[25]
8	Diffusion Approach	$MR = a\exp(-kt) + (1-a)\exp(-kbt)$	[26]
9	Verma et al	$MR = a\exp(-kt) + (1-a)\exp(-gt)$	[27]
10	Midilli et al	$MR = a\exp(-kt^n) + bt$	[28]

color (ranging from 0 for black to 100 for white), while a^* and b^* represent color parameters indicative of the transition from green (+) to red (−) and from yellow (+) to blue (−), respectively [30]. However, it is essential to acknowledge that relying solely on L^*, a^*, and b^* values may not comprehensively capture the perceptual aspects of color for consumers. Consequently, these parameters were utilized in the computation of Chroma (C) and hue angle ($\alpha°$) values, as well as total color differences (ΔE) values, which are pertinent to consumers' color perception Using Eqs. (2), (3) and (4), Chroma (C), hue angle ($\alpha°$) and total color differences (ΔE) values were found respectively [31].

$$C = \sqrt{(a^2 + b^2)} \tag{4}$$

$$\alpha = \tan^{-1}\left(\frac{b}{a}\right) \tag{5}$$

$$\Delta E = \sqrt{(L_0^* - L^*)^2 + (a_0^* - a^*)^2 + (b_0^* - b^*)^2} \tag{6}$$

In this context, the variables L^*, a^*, and b^* represent the color attributes of the dehydrated peach samples, while L_0^*, a_0^*, and b_0^* denote the corresponding color attributes of the fresh peach samples.

Calculation of rehydration capacity

In the investigations aimed at assessing rehydration capacity, the dehydrated peach slices were placed into a beaker filled with purified distilled water, maintaining a

solid–liquid ratio of 1:50, at room temperature for 14 h [32]. Following this period, the rehydrated products were extracted from the beaker, any surplus water was eliminated using filter paper, and their mass was measured on a precision scale. It was performed in 3 replications for each treatment. Rehydration capacity values were calculated with Eq. (7) [33]. In the equation, W_2 is represented as the rehydrated product, while W_1 is defined as the dried product.

$$Rehydration\ \ capacity = \frac{W_2 - W_1}{W_1} \tag{7}$$

Microstructure analysis

For microstructure analysis, the surface sections taken from the same regions of the dried samples were used [34]. After securing the samples onto the sample holder through double-sided tape, a coating procedure is administered, employing a gold–palladium mixture (40/60) in a low-pressure environment. This coating process readies the samples for imaging using Scanning Electron Microscopy (SEM, Carl Zeiss EVO 40 Germany) equipment. Representative microstructural images were acquired at an acceleration voltage of 20 kV.

Data analysis

JMP (Version 7.0, USA) package program was used to analyze the data obtained from the experiments other than modeling. Regression analysis was conducted utilizing the MATLAB software from MathWorks Inc. in the modeling studies. In addition to the primary criterion, which is the correlation coefficient (R^2), the selection of the most suitable equation, considering the variations in the drying curves of the dehydrated samples, also incorporated statistical parameters such as chi-square (χ^2) and root mean square error ($RMSE$). The parameters mentioned above were ascertained utilizing Eqs. (8) and (9) [35]:

$$\chi^2 = \frac{\sum_{=1}^{N} (MR_{\mathrm{exp,i}} - MR_{\mathrm{pre,i}})^2}{N - z} \tag{8}$$

$$RMSE = \sqrt{\frac{\sum_{i=1}^{n} (MR_{\mathrm{pre,i}} - MR_{\mathrm{exp,i}})^2}{N}} \tag{9}$$

In the formula, $MR_{\mathrm{pre,i}}$, $MR_{\mathrm{exp,i}}$, N, and z are defined as the predicted moisture ratio for test number i, the experimental moisture ratio for test number i, the number of experimental data observed, and the number of the independent variable in the model, respectively.

Results and discussion

Drying durations

The moisture content-time curves for the drying of peach samples using three distinct drying methods (EHD, hot air, and EHD-hot air) are presented in Fig. 3. The most extended drying period was documented in the application of EF6.67, with a duration of 720 min, while the briefest drying duration was noted in the EF10-55 °C application, with a duration of 120 min. In the EHD method, increasing the electric field from 6.67 to 10 kV cm^{-1} reduced the drying time by 16.67%. The trend of decreasing drying time with higher voltage values aligns with findings reported by Cao et al. [36]. Comparatively, drying times were found to be longer in the EHD method compared to the hot air method. This outcome aligns with findings reported in the study by Bai et al. [37], wherein the EHD method demonstrated prolonged drying durations compared to hot air drying, as observed in a sludge drying study. Specifically, in the hot air method, drying times were recorded at 290 and 260 min for the 50 and 55 °C drying applications, respectively. This variation is attributed to the increased moisture evaporation at higher temperatures, leading to shorter drying times, a phenomenon supported by Ayadi et al. [38]. The EHD-hot air combination method emerged as the most productive approach for the desiccation of peach samples, with drying times ranging from 200 min (EF6.67–50 °C) to 120 min (EF10-55 °C), as shown in Fig. 3. As discernible from the figure, the augmentation of both temperature and electric field strength resulted in reduced drying durations.

Mathematical modeling

The drying data collected during the desiccation of peach slices utilizing the EHD, hot air and EHD-hot air methods were subjected to fitting against ten distinct thin-layer drying models, as detailed in Table 1. Non-linear regression analysis was employed to estimate the model parameters. The selection of the most appropriate model for characterizing the drying kinetics of peach slices was predicated on criteria involving the highest coefficients of determination (R^2) and the lowest values of both χ^2 and $RMSE$. The statistical outcomes derived from these models are delineated in Table 2 (the hot air and EHD) and Table 3 (the EHD-hot air combination). Upon examining Table 2, it becomes evident that the Midilli et al. model yields the highest R^2 values (ranging from 0.9999 to 0.9996), as well as the lowest $RMSE$ values (0.0028 and 0.0053) and χ^2 values (0.0789×10^{-4} and 0.2834×10^{-4}) for peach slices

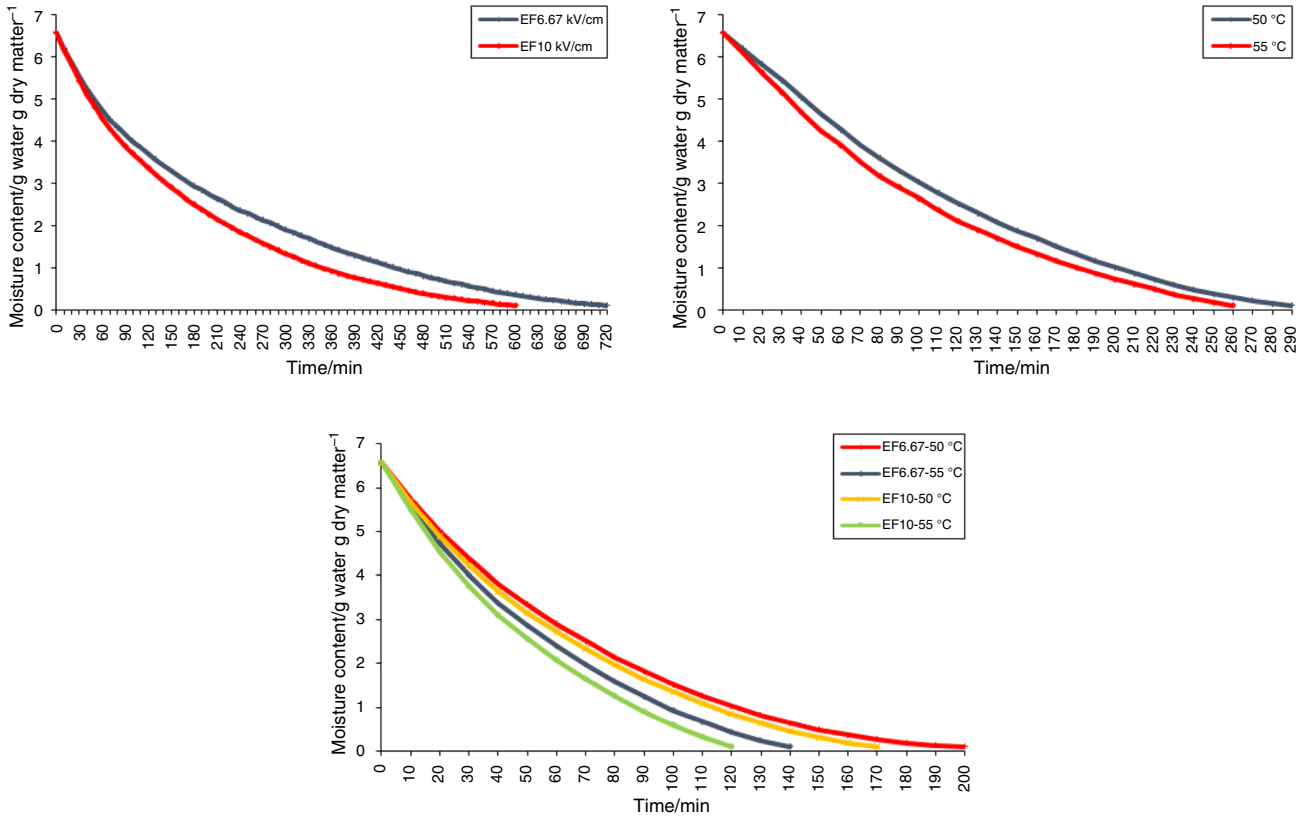

Fig. 3 The moisture content of peach slices dried with the (**a**) EHD, (**b**) Hot air, and (**c**) EHD-hot air combined methods over time

that underwent the EHD and hot air drying methodologies. Table 3 furnishes the statistical outcomes derived from the evaluated models applied to peach samples subjected to the EHD-hot air combination drying process. Notably, the Logarithmic model is the most appropriate for samples dried with the EF6.67–50 °C application, exhibiting an R^2 value of 0.9997, *RMSE* of 0.0053, and χ^2 of 0.2794×10^{-4}. In other EHD-hot air combination applications, the Midilli et al. model consistently offers higher R^2 values across all drying processes and lower *RMSE* and χ^2 values. Figure 4 illustrates the suitability of the Midilli et al. and Logarithmic models for predicting moisture ratios at specific drying times for peach slices dried via the EHD, hot air, and EHD-hot air combination methods. The close alignment between the experimental data and the curves generated by the selected models reinforces their appropriateness for describing the drying characteristics of peach slices under the specified experimental conditions. In line with our study, Doymaz [39], Briki et al. [40], and Karaaslan et al. [3] have also found the Midilli et al. model was identified as the most fitting model for the drying conditions employed in their studies. Similarly, Kingsly et al. [41] found that the Logarithmic model outperformed other models in elucidating the drying kinetics of peach samples, findings consistent with our research.

Color values

Color plays a pivotal role in consumers' product selection and is thus deemed a critical parameter in this context. The preservation of color parameters, particularly following the drying process, is a notable concern. During the drying process, the susceptibility of heat-sensitive bioactive components to temperature variations leads to undesirable consequences, including discoloration and browning of the product [42]. In order to explore this issue, an examination of the color parameters of both fresh and dehydrated peach samples was conducted, employing various drying methodologies, namely, electrohydrodynamic (EHD) drying, hot air drying, and EHD-hot air combination drying, as presented in Table 4. The fresh peach products' initial L^*, a^*, and b^* values were 65.022 ± 0.593, 10.090 ± 0.113, and 48.154 ± 0.487, respectively. Notably, the L^* values exhibited a decrease of 2.81% (at EF6.67) and 15.27% (at 55 °C) due to the drying conditions. This empirical evidence indicates that the dried peach samples possess a darker hue than their fresh counterparts, in line with findings reported by Lima-Corrêa et al. [30]. Additionally, it was noted that the L^* values of products undergoing the EHD drying method surpassed those dried utilizing hot air drying, a trend following the findings reported by Alemrajabi et al. [10] in

Table 2 Statistical analysis results on thin layer drying of peach slices by EHD and hot air method

No	EF6.67 kV cm^{-1}				EF10 kV cm^{-1}				50 °C				55 °C			
	Model Katsayıları	R^2	RMSE	χ^2 (10^{-4})	Model Katsayıları	R^2	RMSE	χ^2 (10^{-4})	Model Katsayıları	R^2	RMSE	χ^2 (10^{-4})	Model Katsayıları	R^2	RMSE	χ^2 (10^{-4})
1	a = 0.9586 k = 0.004237	0.9950	0.0181	3.2831	a = 0.9804 k = 0.005407	0.9977	0.0126	1.5812	a = 1.07 k = 0.009123	0.9857	0.0362	13.0790	a = 1.049 k = 0.01026	0.9905	0.0290	8.3867
2	k = 0.004427	0.9929	0.0217	4.7141	k = 0.005517	0.9973	0.0137	1.8730	k = 0.008519	0.9800	0.0428	18.3473	k = 0.009771	0.9876	0.0330	10.9172
3	k = 0.006137 n = 0.942	0.9942	0.0195	3.8165	k = 0.006136 n = 0.9804	0.9974	0.0134	1.7996	k = 0.002364 n = 1.262	0.9969	0.0168	2.8135	k = 0.004006 n = 1.187	0.9971	0.0160	2.5739
4	a = 0.9805 k = 0.003762 c = −0.04105	0.9966	0.0150	2.2544	a = 0.9956 k = 0.004944 c = −0.03028	0.9988	0.0091	0.8389	a = 1.228 k = 0.006056 c = −0.2089	0.9995	0.0066	0.4321	a = 1.163 k = 0.007407 c = −0.1546	0.9997	0.0095	0.1681
5	a = 0.3429 k_o = 0.00423 b = 0.6144 k_1 = 0.004232	0.9949	0.0184	3.3797	a = 0.03376 k_o = 0.005407 b = 0.9466 k_1 = 0.005406	0.9977	0.0128	1.6367	a = 2.479 k_o = 0.004581 b = −1.462 k_1 = 0.002793	0.9996	0.0058	0.3327	a = 0.9772 k_o = 0.01026 b = 0.07211 k_1 = 0.01026	0.9896	0.0302	9.1156
6	a = 0.6953 k = 0.004973	0.9929	0.0217	4.7211	a = 0.9937 k = 0.005517	0.9973	0.0138	1.9048	a = 1.799 k = 0.01199	0.9962	0.0187	3.4794	a = 1.004 k = 0.009771	0.9871	0.0337	11.3539
7	a = −0.003219 b = 0.000002715	0.9601	0.0514	26.4282	a = −0.003974 b = 0.000004099	0.9699	0.0459	21.0445	a = −0.006319 b = 0.00001021	0.9993	0.0078	0.6144	a = −0.007325 b = 0.00001401	0.9976	0.0145	2.1030
8	a = 0.06283 k = 0.05637 b = 0.07354	0.9957	0.0168	2.8165	a = 0.2309 k = 0.005524 b = 0.9984	0.9972	0.0139	1.9376	a = 0.7349 k = 0.00852 b = 0.9994	0.9785	0.0444	19.7064	a = 0.5536 k = 0.009774 b = 0.9993	0.9866	0.0344	11.8270
9	a = 0.9371 k = 0.004145 g = 0.0562	0.9957	0.0168	2.8165	a = 0.6092 k = 0.005513 g = 0.005523	0.9972	0.0139	1.9376	a = 8.909 k = 0.0145 g = 0.01576	0.9967	0.0174	3.0242	a = 7.331 k = 0.01547 g = 0.01686	0.9973	0.0155	2.4186
10	a = 1.009 k = 0.01264 n = 0.7876 b = −0.0001406	0.9996	0.0053	0.2834	a = 1.002 k = 0.009378 n = 0.8855 b = −0.00009635	0.9998	0.0039	0.1550	a = 1.001 k = 0.004176 n = 1.115 b = −0.0003043	0.9999	0.0037	0.1385	a = 1.003 k = 0.006851 n = 1.045 b = −0.0003342	0.9999	0.0028	0.0789

Table 3 Statistical analysis results on thin layer drying of peach slices by EHD-hot air combined method

No	EF6.67-50 °C				EF6.67-55 °C				EF10-50 °C				EF10-55 °C			
	Model Katsayıları	R^2	RMSE	χ^2 (10^{-4})	Model Katsayıları	R^2	RMSE	χ^2 (10^{-4})	Model Katsayıları	R^2	RMSE	χ^2 (10^{-4})	Model Katsayıları	R^2	RMSE	χ^2 (10^{-4})
1	a = 1.031 k = 0.01523	0.9927	0.0257	6.5882	a = 1.031 k = 0.01863	0.9888	0.0327	10.6264	a = 1.026 k = 0.01623	0.9916	0.0277	7.6352	a = 1.03 k = 0.02088	0.9880	0.0342	11.6602
2	k = 0.01478	0.9919	0.0271	7.3569	k = 0.01806	0.9882	0.0335	11.2407	k = 0.01582	0.9912	0.0283	8.0271	k = 0.02026	0.9876	0.0348	12.0938
3	k = 0.007891 n = 1.143	0.9971	0.0161	2.5989	k = 0.009111 n = 1.165	0.9948	0.0222	4.9276	k = 0.009003 n = 1.131	0.9956	0.0199	3.9773	k = 0.01027 n = 1.168	0.9943	0.0235	5.5411
4	a = 1.097 k = 0.01207 c = −0.09652	0.9997	0.0053	0.2794	a = 1.166 k = 0.01309 c = −0.1719	0.9996	0.0078	0.3312	a = 1.12 k = 0.0122 c = −0.1279	0.9997	0.0051	0.2663	a = 1.186 k = 0.01429 c = −0.1924	0.9997	0.0058	0.3423
5	a = 2.195 k_o = 0.009351 b = −1.198 k_1 = 0.006405	0.9996	0.0063	0.3923	a = 0.8175 k_o = 0.01863 b = 0.2136 k_1 = 0.01862	0.9868	0.0355	12.5582	a = 0.6614 k_o = 0.01623 b = 0.3642 k_1 = 0.01623	0.9904	0.0296	8.7262	a = 0.7316 k_o = 0.02088 b = 0.2987 k_1 = 0.02089	0.9854	0.0378	14.2504
6	a = 1.644 k = 0.01893	0.9974	0.0155	2.4025	a = 1.672 k = 0.02363	0.9950	0.0219	4.8148	a = 1.624 k = 0.0201	0.9959	0.0192	3.6898	a = 1.678 k = 0.02662	0.9944	0.0234	5.4709
7	a = −0.01083 b = 0.00003031	0.9951	0.0212	4.4876	a = −0.01344 b = 0.00004699	0.9963	0.0188	3.5515	a = −0.01176 b = 0.0003613	0.9944	0.0225	5.0705	a = −0.01511 b = 0.00005925	0.9961	0.0195	3.7896
8	a = 9.537 k = 0.0223 b = 1.058	0.9976	0.0148	2.2021	a = 0.4936 k = 0.01804 b = 1.002	0.9863	0.0362	13.1142	a = −9.751 k = 0.02486 b = 0.9533	0.9961	0.0189	3.5793	a = 0.503 k = 0.02026 b = 0.9993	0.9852	0.0381	14.5126
9	a = 8.26 k = 0.02221 g = 0.02372	0.9976	0.0148	2.2036	a = 0.1606 k = 0.01805 g = 0.01806	0.9863	0.0362	13.1142	a = 0.285 k = 0.01582 g = 0.01582	0.9900	0.0302	9.0974	a = 9.091 k = 0.0316 g = 0.0337	0.9944	0.0234	5.4957
10	a = 0.9938 k = 0.01084 n = 1.047 b = −0.0002956	0.9995	0.0069	0.4789	a = 0.9995 k = 0.01615 n = 0.9776 b = −0.000872	0.9998	0.0040	0.1582	a = 0.9987 k = 0.01496 n = 0.9742 b = −0.0005882	0.9998	0.0045	0.1996	a = 1.001 k = 0.0189 n = 0.9589 b = −0.001168	0.9999	0.0033	0.1071

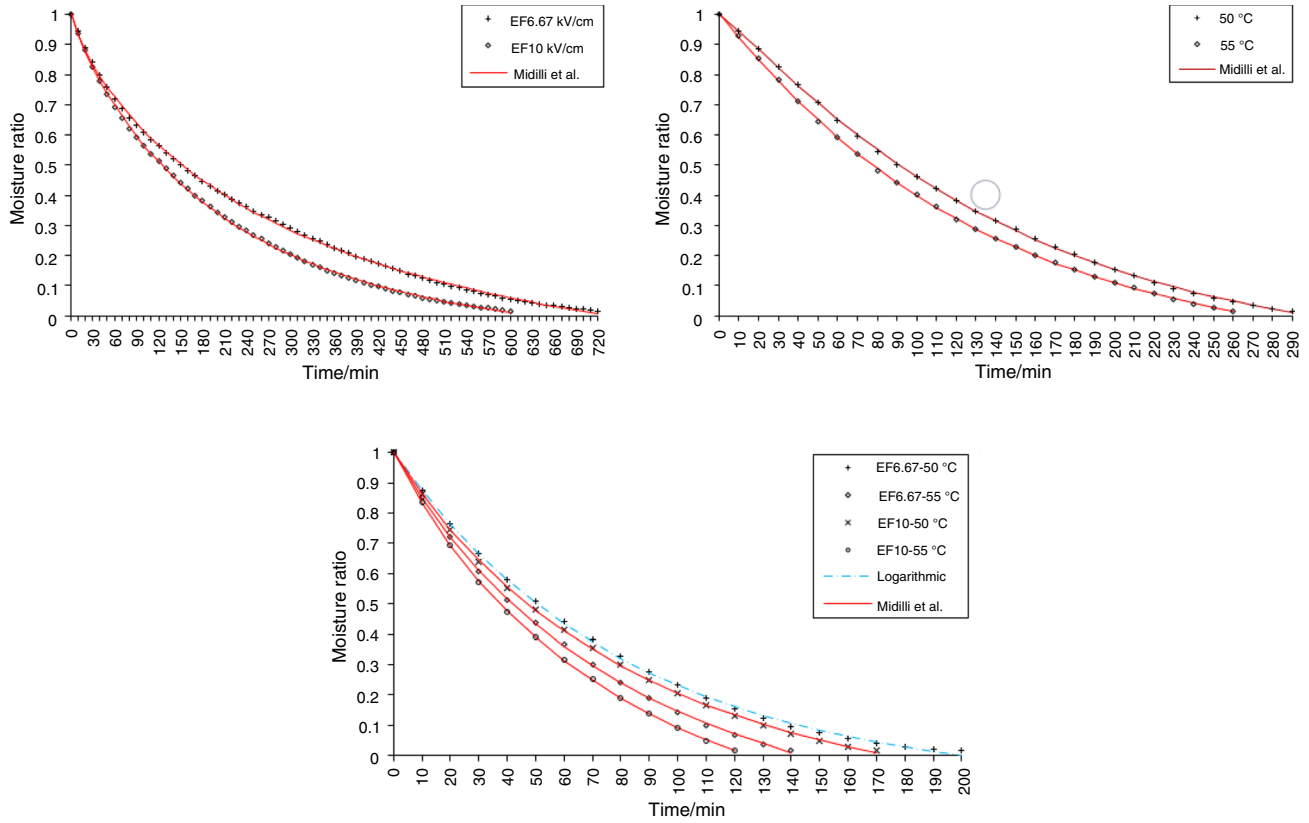

Fig. 4 A comparison of the experimental and theoretical moisture ratios predicted by the Midilli et al. and Logarithmic models under selected drying conditions

Table 4 The color values of fresh and dried peach slices using various drying methods

Drying conditions	Color parameters					
	*L**	*a**	*b**	*C*	*α*°	Δ*E*
Fresh	65.022 (0.593)^{a}	10.090 (0.113)^{g}	48.154 (0.487)^{d}	49.199 (0.487)^{f}	78.205 (0.128)^{a}	–
EHD						
EF6.67 kV cm^{-1}	63.186 (1.392)^{b}	12.834 (0.609)^{f}	51.976 (0.500)^{a}	53.541 (0.360)^{bc}	76.165 (0.752)^{b}	18.268 (0.187)^{a}
EF10 kV cm^{-1}	60.154 (0.426)^{cd}	15.626 (0.638)^{c}	48.304 (1.102)^{d}	50.775 (0.897)^{e}	72.098 (1.013)^{e}	20.609 (0.365)^{c}
Hot air						
50 °C	56.266 (0.066)^{f}	15.382 (0.019)^{c}	50.144 (0.307)^{c}	52.450 (0.294)^{cd}	72.983 (0.095)^{d}	22.538 (0.120)^{d}
55 °C	55.092 (0.319)^{g}	18.470 (0.106)^{b}	51.422 (0.159)^{ab}	54.638 (0.185)^{ab}	70.278 (0.050)^{f}	26.006 (0.034)^{f}
EHD-Hot air						
EF6.67–50 °C	60.806 (0.146)^{c}	14.520 (0.048)^{d}	49.698 (0.784)^{c}	51.776 (0.747)^{de}	73.748 (0.267)^{c}	19.675 (0.239)^{b}
EF6.67–55 °C	59.882 (0.974)^{d}	14.206 (0.133)^{de}	49.562 (0.414)^{c}	51.558 (2.035)^{de}	74.042 (1.145)^{c}	19.726 (0.636)^{b}
EF10-50 °C	59.340 (0.930)^{d}	13.996 (0.521)^{e}	50.240 (2.236)^{bc}	52.162 (0.370)^{d}	74.436 (0.300)^{c}	20.056 (0.392)^{b}
EF10-55 °C	58.268 (0.416)^{e}	19.374 (0.242)^{a}	51.910 (0.816)^{a}	55.408 (0.800)^{a}	69.566 (0.300)^{f}	25.536 (0.462)^{e}

$^{a-g}$Means superscript with different alphabets in the same column differ significantly ($p \leq 0.05$)

their investigation of carrot drying. However, in contrast to our study, Elmizadeh et al. [12] found that the *L** values of the products dried with hot air were higher than those dried with EHD in their quince drying study. It is speculated that the needle-type electrode they used here may have caused this result. Consistent with the observations above, the *a** values of the dried products surpassed those of the fresh samples, signifying a redder coloration in the dried products. It is pertinent to note that the *a** values displayed a positive correlation with both the levels of electric field

strength employed in the EHD method and the temperature parameters set in the hot air drying method, a trend corroborated by the studies conducted by İsmail et al. [43] on nectarine drying using hot air and Dinani et al. [44] on mushroom drying employing the EHD method. In contrast, the b^* values exhibited an inverse relationship with temperature settings in the hot air method and the electric field in the EHD method. The b^* values of the samples showed a decrease with the escalation of the electric field strength in the EHD method and a reduction in temperature within the hot air drying process ($p < 0.05$). Chroma (C) values, representing color saturation, were lowest in the fresh samples but increased due to temperature and electric field settings. The hue angle ($\alpha°$), indicative of the degree of browning, tended to increase with decreased greenness and heightened yellowness [45]. However, this study revealed that elevating the electric field in the EHD method and temperature in the hot air method contributed to a decrease in the hue angle ($\alpha°$). Moreover, the comprehensive color difference (ΔE), a parameter discernible to the human eye and utilized as an indicator of quality in dehydrated products, was scrutinized. Products featuring lower ΔE values were considered more acceptable. Significantly, the products subjected to an electric field strength of 6.67 kV cm^{-1} exhibited the lowest ΔE value, while the highest values were recorded in products subjected to 55 °C. The ΔE values increased with elevated electric field values in the EHD and EHD-hot air combined methods. This trend mirrors the findings of Martynenko and Zheng [46], who asserted that higher voltage levels result in more significant color deterioration, as noted in the apple drying examination. Similarly, an increment in temperature in the hot air method led to an augmentation in ΔE values, a result congruent with Demirel and İsmail's [47] observations in their study on nectarine drying.

Rehydration capacity

The rehydration process, a crucial determinant of drying quality, involves the reconstitution dried products through contact with water. The rehydration ratio indicates the cellular and structural alterations that transpire during the drying process [48]. The extent of rehydration ratio enhancement is contingent upon the preservation of a smooth and intact cellular structure. The rehydration capacity values for peach samples subjected to various drying methods are graphically depicted in Fig. 5. Notably, no statistically significant disparities were discerned in the rehydration capacity values between samples subjected to the EHD method and those desiccated using the EHD-hot air combination technique. On the contrary, it was determined that elevations in temperature within the context of the hot air drying method increased rehydration capacity values. However, this trend did not reach statistical significance ($p > 0.05$).

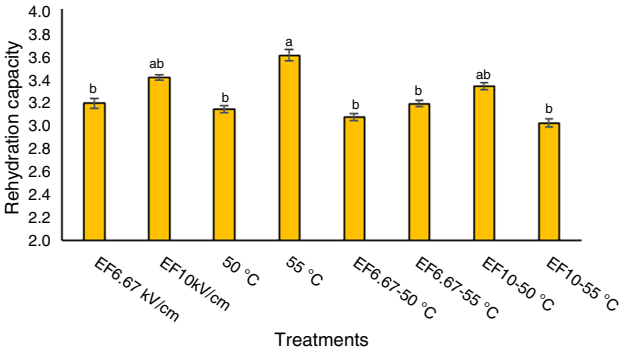

Fig. 5 Rehydration capacity values of peach slices dried under different conditions

This phenomenon is consistent with the findings reported by Doymaz and Bilici [49], who, in their study on peach drying employing hot air at temperatures of 45, 55, 65, and 75 °C, observed an increment in rehydration values for products dried within the range of 45–65 °C. Moreover, the research conducted by Dinani and Havet [50] ascertained that variations in applied voltage did not yield statistically significant differences in rehydration rate values for mushroom samples that were subjected to desiccation under uniform conditions, maintaining a constant temperature of 45 °C and a consistent air velocity. These findings are congruent with our study's outcomes, reinforcing the consistency and validity of the observed trends. In their research, Bai and Sun [51] found that EHD-dried shrimps also showed better rehydration than oven-treated samples and reported that the high temperature applied during the oven-drying process was effective in these findings. In our study, 55 °C hot air drying was higher than the rehydration values of the products dried at 50 °C and EHD. It is predicted that different findings here may be caused by cracks on the product surface.

Microstructure

The scanning electron microscopy (SEM) images presented in Fig. 6 illustrate the alterations in the surface structure of peach samples subjected to eight distinct drying processes, namely, EF6.67, EF10, EF6.67–50 °C, EF6.67–55 °C, EF10-50 °C, EF10-55 °C, 50 °C, and 55 °C. Upon close examination of the micrographs, it becomes evident that peach samples subjected to the hot air drying method exhibited a greater prevalence of surface cracking than those subjected to the EHD drying method. This phenomenon underscores the transformative impact of hot air application on the surface structure of the product [52]. Within the context of the EHD method, it was observed that an elevation in the electric field resulted in a flatter surface with the emergence of small-scale cracks. This observation aligns seamlessly with the outcomes of a study by Yu et al. [53], which found that

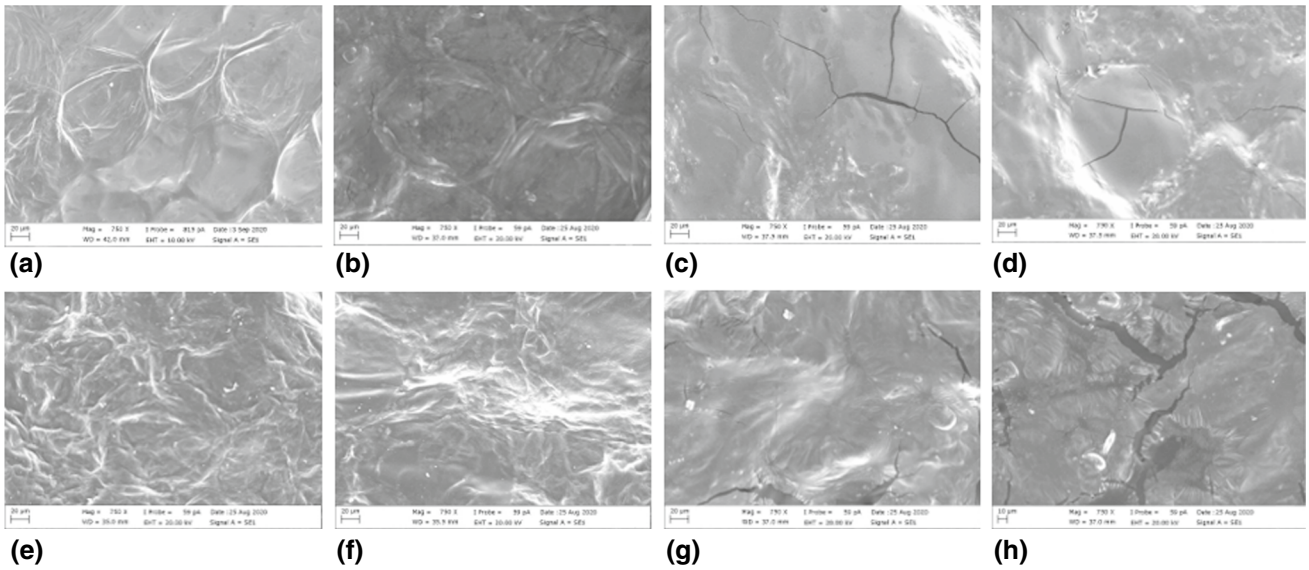

Fig. 6 SEM images of peach slices dried under different drying conditions: (**a**) EF6.67 kV cm^{-1}, (**b**) EF10 kV cm^{-1}, (**c**) 50 °C, (**d**) 55 °C, (**e**) EF6.67-50 °C, (**f**) EF6.67-55 °C, (**g**) EF10-50 °C, and (**h**) EF10-55 °C

increased EHD voltage values led to a heightened occurrence of perforations on the surface of potatoes. Remarkably, the three-dimensional structure of the product's surface remained intact in samples subjected to the combination drying method using EF6.67. However, surface cracking manifested in the samples subjected to the combination drying method employing EF10. Furthermore, a noteworthy distinction emerged when comparing the surfaces of products dried at EF6.67–50 °C and EF6.67–55 °C, wherein no significant disparity was evident. Conversely, the product structure dried at EF10-50 °C exhibited a greater incidence of cracks compared to the product structure dried at EF10-55 °C. This observation resonates with the findings reported by Xie et al. [29], who postulated that cracks may facilitate moisture transfer during drying.

Conclusions

In this study, peach products were dried using three different drying techniques: EHD, hot air, and EHD-hot air drying. The effects of these drying techniques on various parameters such as drying time, mathematical modeling, color characteristics, rehydration capacity, and microstructural properties were investigated. Drying times were the most protracted when employing the EHD method for peach drying. When the EHD application was combined with the hot air method, the drying time of peach was reduced and it was less exposed to hot air. To ascertain the most appropriate thin-layer drying model for the experimental data, ten mathematical models were applied. Subsequently, these models were assessed using the chi-square (χ^2), root mean square of errors (*RMSE*), and coefficient of determination (R^2) as evaluation criteria. The results revealed that among the drying models examined, the models proposed by Midilli et al. showed the highest degree of appropriateness in characterizing the drying kinetics of thin-layer peach slices in all treatments except the EF6.67–50 °C treatment. In the context of color, the L^* values exhibited a decreasing trend with the drying process. In contrast, an increase in electric field within the EHD method and drying temperature within the hot air method led to a rise in ΔE values, signifying increased color deviation. The variation of hot air and electric field had no significant effect on the rehydration capacity of peach samples dried by EHD-hot air and EHD methods. Notably, the most pronounced surface cracks on the product were observed in peach samples subjected to drying conditions involving EF10-55 °C. This showed that a high electric field and high-temperature damage the product surface. This investigation has established that both EHD and EHD-hot air drying methods have the potential to serve as viable alternatives to conventional drying techniques for preserving the quality of agricultural products, thereby meeting consumer expectations. In the future, studies will be conducted in which different temperature and electric field settings are used to determine the optimum drying conditions for peach product drying, energy calculations are made and the nutritional values of the product are examined. In addition, nanofluid technology will be utilized to increase the heat transfer capacity of the device and make it more efficient.

Authors' contribution AP: Data curation, Writing-Original draft preparation, Writing-Reviewing and Editing Conceptualization, Methodology, Software, Visualization, Investigation.

Funding Open access funding provided by the Scientific and Technological Research Council of Türkiye (TÜBİTAK). No funding was received for conducting this study.

Data availability The datasets generated during and/or analyzed during the current study are available from the corresponding author on reasonable request.

Declarations

Conflict of interest The authors have no competing interests to declare that are relevant to the content of this article.

References

1. Khan WA. Significance of magnetized Williamson nanofluid flow for ferromagnetic nanoparticles. Waves Random Complex. 2023. https://doi.org/10.1080/17455030.2023.2207390.
2. Singh A, Vanga SKK, Raveendran Nair G, Gariepy Y, Orsat V, Raghavan V. Electrohydrodynamic drying of sand. Dry Technol. 2017;35(3):312–22. https://doi.org/10.1080/07373937.2016.1170028.
3. Karaaslan S, Ekinci K, Ertekin C, Kumbul BS. Thin layer peach drying in solar tunnel drier. Erwerbs-obstbau. 2021;63(1):65–73. https://doi.org/10.1007/s10341-020-00536-4.
4. El-Mesery HS, Ashiagbor K, Hu Z, Alshaer WG. A novel infrared drying technique for processing of apple slices: drying characteristics and quality attributes. Case Stud Therm Eng. 2023;52:103676. https://doi.org/10.1016/j.csite.2023.103676.
5. Dinani ST, Hamdami N, Shahedi M, Havet M, Queveau D. Influence of the electrohydrodynamic process on the properties of dried button mushroom slices: a differential scanning calorimetry (DSC) study. Food Bioprod Process. 2015;95:83–95. https://doi.org/10.1016/j.fbp.2015.04.001.
6. El-Mesery HS, Farag HA, Kamel RM, Alshaer WG. Convective hot air drying of grapes: drying kinetics, mathematical modeling, energy, thermal analysis. J Therm Anal Calorim. 2023;148(14):6893–908. https://doi.org/10.1007/s10973-023-12195-0.
7. El-Mesery HS. Improving the thermal efficiency and energy consumption of convective dryer using various energy sources for tomato drying. Alex Eng J. 2022;61(12):10245–61. https://doi.org/10.1016/j.aej.2022.03.076.
8. Defraeye T, Martynenko A. Future perspectives for electrohydrodynamic drying of biomaterials. Dry Technol. 2018;36(1):1–10. https://doi.org/10.1080/07373937.2017.1326130.
9. Defraeye T, Martynenko A. Electrohydrodynamic drying of food: new insights from conjugate modeling. J Clean Prod. 2018;198:269–84. https://doi.org/10.1016/j.jclepro.2018.06.250.
10. Alemrajabi AA, Rezaee F, Mirhosseini M, Esehaghbeygi A. Comparative evaluation of the effects of electrohydrodynamic, oven, and ambient air on carrot cylindrical slices during drying process. Dry Technol. 2012;30(1):88–96. https://doi.org/10.1080/07373937.2011.608913.
11. Bai Y, Qu M, Luan Z, Li X, Yang Y. Electrohydrodynamic drying of sea cucumber (*Stichopus japonicus*). LWT-Food Sci Technol. 2013;54(2):570–6. https://doi.org/10.1016/j.lwt.2013.06.026.
12. Elmizadeh A, Shahedi M, Hamdami N. Quality assessment of electrohydrodynamic and hot-air drying of quince slice. Ind Crops Prod. 2018;116:35–40. https://doi.org/10.1016/j.indcrop.2018.02.048.
13. Wang JR, Wu XY, Cui CB, Bi JF. Effect of osmotic dehydration combined with vacuum freeze-drying treatment on characteristic aroma components of peach slices. Food Chem X. 2024. https://doi.org/10.1016/j.fochx.2024.101337.
14. Guo C, Bi J, Li X, Lyu J, Xu Y, Hu J. Investigation on the phenolic composition, related oxidation and antioxidant activity of thinned peach dried by different methods. LWT. 2021;147:111573. https://doi.org/10.1016/j.lwt.2021.111573.
15. Wang J, Sheng K. Far-infrared and microwave drying of peach. LWT-Food Sci Technol. 2006;39(3):247–55. https://doi.org/10.1016/j.lwt.2005.02.001.
16. Nasri F. Solar thermal drying performance analysis of banana and peach in the region of Gafsa (Tunisia). Case Stud Therm Eng. 2020;22: 100771. https://doi.org/10.1016/j.csite.2020.100771.
17. Chatzilia T, Kaderides K, Goula AM. Drying of peaches by a combination of convective and microwave methods. J Food Process Eng. 2023;46(4): e14296. https://doi.org/10.1111/jfpe.14296.
18. Delgado T, Pereira JA, Casal S, Ramalhosa E. Effect of drying on color, proximate composition and drying kinetics of sliced chestnuts. J Food Process Eng. 2016;39(5):512–20. https://doi.org/10.1111/jfpe.12244.
19. Caliskan G, Dirim SN. Drying characteristics of pumpkin (*Cucurbita moschata*) slices in convective and freeze dryer. Heat Mass Transf. 2017;53(6):2129–41. https://doi.org/10.1007/s00231-017-1967-x.
20. Pirnazari K, Esehaghbeygi A, Sadeghi M. Modeling the electrohydrodynamic (EHD) drying of banana slices. Int J Food Eng. 2016;12(1):17–26. https://doi.org/10.1515/ijfe-2015-0005.
21. Sacilik K, Unal G. Dehydration characteristics of Kastamonu garlic slices. Biosyst Eng. 2005;92(2):207–15. https://doi.org/10.1016/j.biosystemseng.2005.06.006.
22. Amiri Chayjan R, Shadidi B. Modeling high-moisture Faba bean drying in fixed and semi-fluidized bed conditions. J Food Process Preserv. 2014;38(1):200–11. https://doi.org/10.1111/j.1745-4549.2012.00766.x.
23. Bhattacharya M, Srivastav PP, Mishra HN. Thin-layer modeling of convective and microwave-convective drying of oyster mushroom (*Pleurotus ostreatus*). J Food Sci Technol. 2015;52(4):2013–22. https://doi.org/10.1007/s13197-013-1209-2.
24. Ergün K, Çalışkan G, Dirim SN. Determination of the drying and rehydration kinetics of freeze dried kiwi (*Actinidia deliciosa*) slices. Heat Mass Transf. 2016;52(12):2697–705. https://doi.org/10.1007/s00231-016-1773-x.
25. Belghith A, Azzouz S, ElCafsi A. Desorption isotherms and mathematical modeling of thin layer drying kinetics of tomato. Heat Mass Transf. 2016;52(3):407–19. https://doi.org/10.1007/s00231-015-1560-0.

26. Perea-Flores MJ, Garibay-Febles V, Chanona-Perez JJ, Calderon-Dominguez G, Mendez-Mendez JV, Palacios-González E, Gutierrez-Lopez GF. Mathematical modelling of castor oil seeds (*Ricinus communis*) drying kinetics in fluidized bed at high temperatures. Ind Crops Prod. 2012;38:64–71. https://doi.org/10.1016/j.indcrop.2012.01.008.
27. Taşkın O, İzli G, İzli N. Convective drying kinetics and quality parameters of European cranberrybush. J Agric Sci. 2018;24(3):349–58. https://doi.org/10.15832/ankutbd.456654.
28. Midilli A, Kucuk H, Yapar Z. A new model for single-layer drying. Dry Technol. 2002;20(7):1503–13. https://doi.org/10.1081/DRT-120005864.
29. Xie L, Zheng ZA, Mujumdar AS, Fang XM, Wang J, Zhang Q, Ma Q, Xiao WH, Liu YH, Gao ZJ. Pulsed vacuum drying (PVD) of wolfberry: Drying kinetics and quality attributes. Dry Technol. 2018;36(12):1501–14. https://doi.org/10.1080/07373937.2017.1414055.
30. Lima-Corrêa RDAB, dos Santos Andrade M, Freire JT, do Carmo Ferreira M. Thin-layer and vibrofluidized drying of basil leaves (*Ocimum basilicum* L.): analysis of drying homogeneity and influence of drying conditions on the composition of essential oil and leaf colour. J Appl Res Med Aromat Plant 2017;7:54–63. https://doi.org/10.1016/j.jarmap.2017.05.001.
31. Guiné RP, Barroca MJ. Effect of drying treatments on texture and color of vegetables (pumpkin and green pepper). Food Bioprod Process. 2012;90(1):58–63. https://doi.org/10.1016/j.fbp.2011.01.003.
32. Vásquez-Parra JE, Ochoa-Martínez CI, Bustos-Parra M. Effect of chemical and physical pretreatments on the convective drying of cape gooseberry fruits (*Physalis peruviana*). J Food Eng. 2013;119(3):648–54. https://doi.org/10.1016/j.jfoodeng.2013.06.037.
33. Aydogdu A, Sumnu G, Sahin S. Effects of microwave-infrared combination drying on quality of eggplants. Food Bioproccess Technol. 2015;8(6):1198–210. https://doi.org/10.1007/s11947-015-1484-1.
34. Xie L, Mujumdar AS, Fang XM, Wang J, Dai JW, Du ZL, Xiao HW, Liu Y, Gao ZJ. Far-infrared radiation heating assisted pulsed vacuum drying (FIR-PVD) of wolfberry *(Lycium barbarum* L): Effects on drying kinetics and quality attributes. Food Bioprod Process. 2017;102:320–31. https://doi.org/10.1016/j.fbp.2017.01.012.
35. Meziane S. Drying kinetics of olive pomace in a fluidized bed dryer. Energy Convers Manag. 2011;52(3):1644–9. https://doi.org/10.1016/j.enconman.2010.10.027.
36. Cao W, Nishiyama Y, Koide S. Electrohydrodynamic drying characteristics of wheat using high voltage electrostatic field. J Food Eng. 2004;62(3):209–13. https://doi.org/10.1016/S0260-8774(03)00232-2.
37. Bai YX, Shi H, Yang YX. Application of electrohydrodynamic drying technology in sludge. Adv Mat Res. 2012;424:61–4. https://doi.org/10.4028/www.scientific.net/AMR.424-425.61.
38. Ayadi M, Mabrouk SB, Zouari I, Bellagi A. Kinetic study of the convective drying of spearmint. J Saudi Soc Agric Sci. 2014;13(1):1–7. https://doi.org/10.1016/j.jssas.2013.04.004.
39. Doymaz I. Suitability of thin-layer drying models for infrared drying of peach slices. J Food Process Preserv. 2014;38(6):2232–9. https://doi.org/10.1111/jfpp.12277.
40. Briki S, Zitouni B, Bechaa B, Amiali M. Comparison of convective and infrared heating as means of drying pomegranate arils (*Punica granatum* L.). Heat Mass Transf. 2019;55(11):3189–99. https://doi.org/10.1007/s00231-019-02644-8.
41. Kingsly RP, Goyal RK, Manikantan MR, Ilyas SM. Effects of pretreatments and drying air temperature on drying behaviour of peach slice. Int J Food Sci Technol. 2007;42(1):65–9. https://doi.org/10.1111/j.1365-2621.2006.01210.x.
42. Poojitha P, Athmaselvi KA. Effect of ohmic blanching on drying kinetics, physicochemical and functional properties of garlic powder. J Food Sci Technol. 2020. https://doi.org/10.1007/s13197-020-04676-z.
43. İsmail O, Beyribey B, Doymaz İ. Effect of drying methods on drying characteristic, energy consumption and color of nectarine. J Therm Eng. 2016;2(3):801–6.
44. Dinani ST, Hamdami N, Shahedi M, Havet M. Quality assessment of mushroom slices dried by hot air combined with an electrohydrodynamic (EHD) drying system. Food Bioprod Process. 2015;94:572–80. https://doi.org/10.1016/j.fbp.2014.08.004.
45. Shingare SP, Thorat BN. Effect of drying temperature and pretreatment on protein content and color changes during fluidized bed drying of finger millets (Ragi, *Eleusine coracana*) sprouts. Dry Technol. 2013;31(5):507–18. https://doi.org/10.1080/07373937.2012.744033.
46. Martynenko A, Zheng W. Electrohydrodynamic drying of apple slices: energy and quality aspects. J Food Eng. 2016;168:215–22. https://doi.org/10.1016/j.jfoodeng.2015.07.043.
47. Demirel FM, Ismail O. Investigation of the effect of a hybrid drying method on the color quality of nectarine slices and energy consumption. Stud Univ Babes-Bolyai Chem. 2017;62(1):237–48. https://doi.org/10.24193/subbchem.2017.1.21.
48. Aversa M, Curcio S, Calabrò V, Iorio G. Experimental evaluation of quality parameters during drying of carrot samples. Food Bioprocess Technol. 2012;5(1):118–29. https://doi.org/10.1007/s11947-009-0280-1.
49. Doymaz İ, Bilici B. Influence of citric acid pretreatment on drying of peach slices. Int J Food Eng. 2014;10(4):829–37. https://doi.org/10.1515/ijfe-2014-0026.
50. Dinani ST, Havet M. Effect of voltage and air flow velocity of combined convective-electrohydrodynamic drying system on the physical properties of mushroom slices. Ind Crops Prod. 2015;70:417–26. https://doi.org/10.1016/j.indcrop.2015.03.047.
51. Bai YX, Sun B. Study of electrohydrodynamic (EHD) drying technique for shrimps. J Food Process Preserv. 2011;35(6):891–7. https://doi.org/10.1111/j.1745-4549.2011.00542.x.
52. Xiao HW, Gao ZJ, Lin H, Yang WX. Air impingement drying characteristics and quality of carrot cubes. J Food Process Eng. 2010;33(5):899–918. https://doi.org/10.1111/j.1745-4530.2008.00314.x.
53. Yu H, Bai A, Yang X, Wang Y. Electrohydrodynamic drying of potato and process optimization. J Food Process Preserv. 2018;42(2): e13492. https://doi.org/10.1111/jfpp.13492.